

LUND UNIVERSITY

SOLID STATE PHYSICS

Reactive Ion Etching of Silicon using F-based chemistry -
Exploring the Limits

Author:
Harald HAVIR

Supervisor:
Ivan MAXIMOV



LUND
UNIVERSITY

Abstract

Dry Etching is widely used in nanoprocessing as a method of pattern transfer onto a hard substrate, like silicon. Improving the resolution of this etch process is an important step in reducing the feature size in, for instance, computer microchips, or Nanoimprint Lithography stamps.

The Reactive Ion Etcher at Lund University has recently been upgraded with a turbo molecular pump. This allows for lower pressure ranges with any given gas flow in the working chamber. Therefore, a sufficient process window had to be established for the upgraded system, where a plasma can be generated and sustained in a stable manner. The study shows that the process window for the system appears to be large, with power, pressure and flow rates not hindering plasma generation outside of hardware limitations.

A recipe for anisotropic etching was developed and, although limited in etch rates and mask selectivity, the process shows promise as anisotropic structures as small as 30 nm were successfully etched with anisotropic features.

Acronyms and Abbreviations

RIE	Reactive Ion Etching
SEM	Scanning Electron Microscope
LNL	Lund Nano Lab
RF	Radio Frequency
NIL	Nano Imprint Lithography
E-field	Electric Field
sccm	Cubic centimeters per minute

Contents

Acronyms and Abbreviations	ii
1 Introduction	1
2 Theory	1
2.1 Plasma Physics & Generation	1
2.2 Dry Etching in Nanoprocessing	2
2.3 Reactive Ion Etching	3
2.3.1 Silicon Etching	3
2.3.2 Chemical Etching	3
2.3.3 Ion Bombardment	4
2.4 Characteristics of RIE	4
2.4.1 Polymerization	4
2.4.2 Selectivity	5
2.4.3 Anisotropy and Aspect Ratio	5
2.4.4 Aperture Effects	5
3 Method	5
3.1 Machines	5
3.1.1 Trion system	5
3.1.2 Loading Effects	6
3.1.3 Temperature Control	6
3.1.4 Optical Microscope	6
3.1.5 Ellipsometer	6
3.1.6 Scanning Electron Microscope	7
3.2 Plasma Parameter Study	7
3.3 Etching	9
3.3.1 Sample Preparation and Handling	9
3.3.2 Sample Etching in 8 : 20 sccm of SF ₆ :CHF ₃	10
3.3.3 Preconditioned Etch Chamber	11
3.3.4 Sample Etching in 6 : 24 sccm of SF ₆ :CHF ₃	11
3.3.5 High Resolution Samples	11
4 Results and Analysis	11
4.1 Parameter study	12
4.2 Etch Tests	15
4.2.1 Etching in 8:20 sccm of SF ₆ :CHF ₃	15
4.2.2 Etching in 6:24 sccm of SF ₆ :CHF ₃	17
4.2.3 Preconditioning	18
4.2.4 High Resolution Lines Sample	19
5 Discussion	21
5.1 Methodology Errors	21
5.2 Measurement Errors	22
6 Conclusion and Outlook	23
7 Acknowledgements	24

1 Introduction

Etching has long been used in micro fabrication as a means of pattern transfer for the purposes of creating integrated circuits [1] used in every piece of modern technology. Originally, a chemical wet etching could quickly transfer features from a masking material to a silicon substrate, using the crystalline pattern as an etching guide to achieve the desired etch directionality. However, as features kept shrinking, the wet etch method produced too large deviations due to the isotropic nature of the etch. Dry (or Plasma) etching was implemented as an alternative in the 1960s.

This method utilized the properties of a plasma to generate reactive species that could etch the surface with a higher selectivity and etch directionality than its counterpart. The ability to utilize ionized species inside the plasma in conjunction with the high mobility of free electrons to produce a directional bombardment of the substrate surface became an easy way to improve etch directionality in a dry etching method called Reactive Ion Etching (RIE). For a more detailed history of plasma etching, please read the review article "Plasma etching: Yesterday, Today, and Tomorrow" -Vincent M. Donnelly and Avinoam Kornblit [2]

This thesis paper will focus on the Trion Sirius T2 RIE in the Lund Nano Lab (LNL). This etcher has recently been upgraded with an additional turbo molecular pump in series with the previous backing pump. This enhanced the ability to work at low pressures, and made larger gas flows available for all ranges of pressure. This newly opened process window allows etching to occur at pressures as low as 5 mTorr, but it has been unknown where the boundaries of this process window lies. The main focus of this thesis is to showcase the existence and location of these boundaries for the LNL etcher. Following this, an etch recipe used by a previous research team in this pressure range will be studied and altered so as to hopefully achieve anisotropic etching of silicon.

2 Theory

2.1 Plasma Physics & Generation

Plasma is commonly referred to as the fourth state of matter and naturally occurs inside stars. It is most easily described as a highly ionized gas, where no strong bonds exist between the charged particles in the plasma. A plasma is thus generated by exciting a gas to the level where a significant ionization of the species has occurred. This can be done by thermal ionization, where a temperature of above (around) 5000 K is necessary to provide ionization levels of energy to the gas. Alternatively, the plasma can be generated by means of an electric field.

In order to generate a plasma electrically, one utilizes the fact that in any gas there is a small amount of free electrons and ionized atoms due to ionization from cosmic background radiation. Once an electric field is applied, these charged particles will be accelerated and collide with other gas atoms. Once a sufficient energy threshold is attained, the collisions will have enough energy to further ionize the gas, causing a chain reaction where the number of free electrons multiply. This can be expressed with the reaction



This interaction describes how any molecule (M) may be hit with an energized electron (e^*) result in an ionized molecule (M^+) and an additional electron.

Due to the plasma constituents being charged, a DC field would cause a separation of charges. More useful is to utilize an oscillating electric field (E-field). High frequency oscillations (in the order of Megahertz) are used to keep the plasma contained and stable. In such a system the free electrons will accelerate back and forth and, with sufficient power in the E-field, will have enough energy to ionize the gas and ignite a plasma. Further increasing the power of the E-field will cause a higher concentration of plasma relative to gas, as more energy is made available for ionization.

In a plasma generated this way the majority of the gas is relatively cool, with only the electrons reaching energies between 1 - 10 eV (10^4 - 10^5 K). Due to the overall low concentration of energetic electrons, the plasma over all is at room temperature. It is therefore called a Cold Plasma.

Due to the mobility of electrons relative to the ions, a plasma which comes into contact with matter will have a large amount of electrons diffuse into the solid surface due to statistical effects. This will cause a self-bias between the plasma and the surface which forces the positively charged ions to accelerate downwards, perpendicularly to the surface [3]. It is this effect, (which will be further discussed in section 2.3.3), that gives plasma etching its high anisotropy.

Contrary to what has been implied previously, an electrically stimulated plasma does not only contain ionized molecules and electrons. It rather contains a large variety of particles that have been created as a result of collisions either breaking or creating molecular bonds. For instance, in this experimental work, a gas combination of SF₆ and CHF₃ is used as the *etching gas*. In a plasma from this gas mixture, a large part of molecules will be ionized by reaction 1, this being the reaction that sustains the plasma. However, other reactions can also take place due to high energy collisions. For instance, as a result of a collision a molecular bond can be broken, creating a free atom (A) and a different molecule remnant.



In the given gas mixture, this second interaction is very interesting, as it is responsible for releasing the *free radical F·* (with the "." representing the missing valence electron). This same reaction is also responsible for the creation of CF₂ which can polymerize by forming long C_nF_{2n} chains. Fortunately enough, all of these components have a use in the etching process which will be detailed in the following sections [4]

2.2 Dry Etching in Nanoprocessing

Dry Etching is a collective term for processes which produce an etching effect without the use of liquids. Generally speaking, this etching process is done by a plasma. Such etch processes are collectively called Plasma Etching, and various methods of plasma etching exist. A very basic set up has a chamber filled with gas, in which two electrodes are placed. A strong DC field is then produced between the electrodes until a discharge propagates through the gas. This excites the gas molecules to produce reactive species which can chemically etch the substrate. In order to generate patterns from etching, a masking material is applied on the substrate and patterned

to the desired shape. This mask prevents etching from taking place and means that a pattern can be transferred into hard substrates such as semiconductors or metals.

2.3 Reactive Ion Etching

RIE is the most commonly used type of plasma etching and uses a Radio Frequency (RF) source to generate the plasma. The electron cascading process described earlier creates a large amount of highly mobile electrons which diffuse and recombine with nearby solids. This causes positive ions to accelerate and bombard the surface, providing an anisotropic etching component in addition to the chemical etch. This concept can be further built upon by for instance using an inductively coupled plasma source separate from the RF generator to allow more individual control over plasma density and ion bombardment energy.

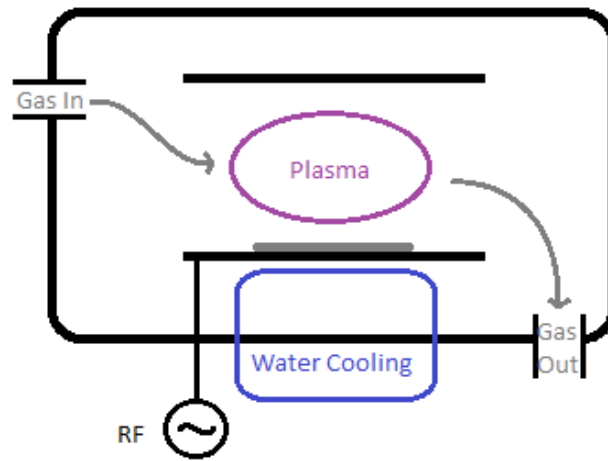


Figure 1: A simple schematic of a RIE system

2.3.1 Silicon Etching

RIE can be used to etch a large variety of materials among semiconductors and metals. This focus of this thesis, however, lies on the etching of silicon. The methods used when etching silicon utilize the fact that Si-Si bonds can be broken if any energetically favorable options appear. If the rest products of this chemical reaction has a high vapor pressure, they will easily desorb from the surface and thus make space for more interactions [5]. The chemicals which display these features are the halogen gases: Fluorine, Chlorine and occasionally Bromine.

2.3.2 Chemical Etching

The gases are inserted into the plasma chamber in the form of a relatively chemically inert gas where reaction 2 breaks the molecular bonds and creates atomic radicals. These radicals are uncharged and will thus move in a random way, meaning that they interact equally with each surface of the substrate. The radicals will break Si-Si bonds and attach themselves to the silicon and create a new compound which is free to drift off from the substrate. With Fluorine as the etching gas, this final product is

SiF_4 . This etching process is isotropic, but does not attack an appropriately selected etch mask. In other words, the *Selectivity* of this process is large (see section 2.4.2).

2.3.3 Ion Bombardment

The other etching component is the so called ion bombardment which is caused by the self-bias effect mentioned earlier. This ion bombardment is mostly perpendicular to the surface, but at higher pressures the mean free path of the ions is short enough that collisions may cause less direct bombardment. The results of this effect is a substrate-wide energy deposit which breaks bonds between substrate atoms and sputters away the surface. This is done all over the substrate, and does not necessarily discriminate between substrate and etching mask. A hard mask, such as Chromium, has a high resistance to the sputtering effects, which yields a high selectivity. However, a soft mask, such as resist, will be sputtered with the same rate as the substrate, meaning that the ion bombardment has a low selectivity in those conditions.

The sputtering rate can be directly correlated to the power of the E-field. Because a higher power generates a larger plasma density, this also means that there are more electrons which can diffuse, in turn generating a higher DC bias towards the substrate. This control of the ion bombardment is necessary if one wants to optimize the selectivity to a soft mask.

The reason that ion bombardment is so useful was shown by J. W. Coburn and Harold F. Winters [6]. They show that the etching rates of the two separate processes (chemical etching and sputtering) are small compared to the etch rate of both processes acting together. This is due to a combination of effects, for instance energy being deposited and thus allowing easier formation of SiF_4 .

2.4 Characteristics of RIE

2.4.1 Polymerization

Despite the ion bombardment only enhancing etching perpendicular to the surface, the chemical component does etch isotropically and can contribute with some amount of undercut of the etch mask. In order to minimize this, the fact that CF_2 polymers can be created by introducing a carbon-containing gas into the gas mixture is utilized. These polymer chains will, just like free radicals, deposit themselves onto any and all surfaces uniformly, creating a thin polymer layer which is inert with respect to free fluorine, but can be broken by the highly energetic ion bombardment. This effectively protects the sidewalls from being etched away, but does slow down the total etch rate. Having too high rates of polymerization will thus lead to severely reduced etch rates, whereas too low deposition rates will yield insufficient protection of the sidewalls and cause some horizontal etching to take place. The rate of polymerization can be controlled by adjusting the ratio of carbon to fluorine in the plasma. Increasing the carbon-containing gas rate will yield higher polymerization rate.

2.4.2 Selectivity

Selectivity is the ratio of the etch rate of the substrate to the etch rate of the mask.

$$S = \nu_s/\nu_m \quad (3)$$

For any set of parameters that yield a low selectivity, the etch depth is limited entirely by the mask thickness. This means that obtaining a sufficient selectivity is essential. When using a hard mask, the selectivity is determined by any chemical component that can etch the mask. A soft mask on the other hand, such as resist, is also etched by sputtering. When etching with a soft mask, increasing the selectivity can be done by reducing the effects of sputtering in the absence of chemical reactions. This can be done by allowing polymerization, as the continuously refreshing polymer layer absorbs some of the ion bombardment. This will, however, reduce the etch rate of the substrate as well.

2.4.3 Anisotropy and Aspect Ratio

Anisotropy is a measure of the perpendicular etch rate compared to the lateral etch rate. An anisotropic etch will have sidewalls perpendicular to the substrate or an outwards slope, away from the mask edge. An isotropic etch will be easily identified by a sidewall profile which curves in under the masking material.

Aspect ratio is defined as the ratio between etch depth and etch height and can also be an important measurement of the etching capabilities of a specific process. A process can have a low aspect ratio but high anisotropy for instance if no horizontal etching takes place but the polymerization causes outwards sloping sidewalls. An ideal pillar or hole has both high anisotropy and a high aspect ratio.

2.4.4 Aperture Effects

When etching deep or narrow structures, one has to consider the increased difficulty in supplying reactive species to the bottom of the structure. For a deep hole, the relative size of the hole diameter compared to the hole depth is smaller than for a shallow and wide hole. The solid angle of straight paths leading to the bottom of the pit decreases with etch depth, until a certain minimum has been achieved.

3 Method

3.1 Machines

3.1.1 Trion system

The Trion RIE system, Sirius T2 Tabletop RIE (henceforth only referred to as the "Trion System"), manufactured by Trion Tech [7], was the main machine of relevance in this thesis. The main component is a vacuum chamber with two electrodes, one placed at the bottom of the chamber, and one on an openable lid. The electrodes have a diameter of 20 cm. The system backing pump was also connected in series with a new turbo molecular pump which enhanced the low-pressure pumping rate. It is also connected to a gas supply which can provide varying amounts of CF_4 , CHF_3 , SF_6 , Ar , and O_2 . One gas line with N_2 is available, but is only used when purging the vacuum and is unavailable for processes.

The system is controlled by using the accompanying software installed on a Windows XP machine which is attached to the system. The software allows the user control over the following variables: time [s], RF power [W], gas flow [sccm] (cubic centimeters per minute), as well as chamber pressure [mTorr]. The system also provides real-time measurements for: time, RF power forward and RF power reflected, gas flow, chamber pressure, DC bias [V] (see section 2.3.1), and lastly a small viewing window which can be used to observe the plasma glow inside the chamber. The system was also equipped with two variable capacitors to help adjust for impedance differences in order to minimize the reflected RF power. These can be adjusted manually or automatically. For the purposes of this project, the capacitors were set to auto adjust.

The system allows the user to either create recipes with predefined chamber settings to allow for identical etch conditions each time, as well as a manual control where the user has real-time control over each parameter and can change the settings on the fly.

3.1.2 Loading Effects

During the etching process, the amount of material to etch has an effect on the gas composition, as a larger amount of silicon being removed causes a faster depletion of Fluorine radicals [4]. These loading effects can be manipulated by adding additional silicon into the chamber during the etching process, for instance a bare silicon wafer, as shown in previous research on the local system [8]. If loading effects are present, the chemical etch rate is limited by the total flow rate of gas. This means that total gas flow rate in such a system has an effect on isotropic etch rate. Conversely, increasing loading effects by inserting a larger total area of silicon in the etching chamber will increase anisotropy of the etch profile.

3.1.3 Temperature Control

Due to the energy deposition from ion bombardment, the silicon wafer can be heated significantly. A high temperature has been shown to severely limit the anisotropy of the etching process [8]. A good thermal conductivity to the water cooled base plate of the etching system can therefore improve the etching results. As the samples were placed on a small piece of thermally conductive sticky tape which separated it from the underlying silicon wafer, the thermal conductivity should ideally not have been hampered.

3.1.4 Optical Microscope

In order to observe samples to discern whether patterning and etching had occurred, an optical microscope was used. This microscope has a range of magnifications between 25x and 1000x with manual focusing of the lenses.

3.1.5 Ellipsometer

The best way to measure the thickness of etch mask is by using an ellipsometer. The ellipsometer works by shooting a range of wavelengths of light onto a sample and analyzing the polarization of the reflected light for different incident angles. This change in polarization reveals information about the different layers of the sample, including the thickness of the mask.

To make a measurement, the sample is placed in front of the light beam on top of a platform, which is manually adjusted to the correct position.

3.1.6 Scanning Electron Microscope

In order to closely observe structures on the 10-500 nm scale, a Scanning Electron Microscope (SEM) was used. The SEM works by focusing an electron beam onto the sample with a raster scan. Secondary electrons are then produced and detected. These secondary electrons are used to form the SEM image. This can produce images with a resolution large enough to distinguish features on a nanometer scale.

The SEM has a main vacuum chamber, inside which the electron column lies. Secondary electron detectors are installed. Outside of this main vacuum chamber is a load lock where pressure can be altered between atmospheric pressure and vacuum. The load lock is sealed off from the main chamber by a vacuum sealed door which can be opened and close when both sides are under a vacuum.

Once the sample is inside the SEM, the software allows the user control over the position and tilt of the stage. To achieve the optimal focus, one has control over five parameters: the focus, stigmator (x, y), apperture align (x, y), the probe current and acceleration voltage of electrons.

3.2 Plasma Parameter Study

As the Trion system had been equipped with a new turbo molecular pump in series with its previous backing pump, it could now operate at much lower pressures than before. However, this previously uncharted region of chamber settings could contain regions where plasma generation would fail or, once successful, not keep the plasma stable.

The first limit that was studied was therefore the maximum gas flow for any given pressure. This was done in the manual setting of the machine with power and pressure fixed. The gas flow rate was increased from below in steps of 5 sccm until the pressure read-value was larger than or equal to the set value. If the recorded value was larger, the flow rate was decreased until the two values matched. This contributes a small error to the measurement process which is accounted for in the results. The RF power was then turned on to verify that plasma could be generated. If a plasma was generated, it was left ignited for one minute to verify that it was not flickering, followed by cleaning the chamber. Next, the set pressure was increased and the study repeated. This was done for the pressure 1, 5, 10, 15, 20, 25 mTorr at constant power (25 W) and flow rates (10:10 SF₆:CHF₃). This flow rate was used as it has been shown that anisotropic etching with SF₆ and CHF₃ occurs with a ratio of CHF₃ larger than or equal to 50 % [10]. This yielded a data set from which one can extrapolate the maximum flow rate for any given pressure.

It should be noted that whenever it is mentioned that the chamber is cleaned, the parameters detailed in Table 1 were used unless anything else is stated. A dirty chamber is characterized by a significant readout on the reflected RF power, and can change the ability to generate and maintain plasma.

Table 1: The standard recipe used when cleaning chamber. Step two and three should be adjusted so that they each last 1.5 times the etching time for longer etching processes. This is the default cleaning process used unless anything else is mentioned.

Procedure Step	1	2	3
Time	10 s	5 min	5
Power [W]	0	150	75
Pressure [mTorr]	500	500	250
CF_4 rate [sccm]	100	25	0
O_2 rate [sccm]	0	25	15

In order to identify the process window, a large scale parameter study in three dimension was considered with adjustable power, pressure, and (total) gas flow. The idea was to set flow rate and pressure, while decreasing power down to a minimum, then re-doing the experiment with lower pressures after cleaning the chamber. After having gone through the range of pressures, the process would be repeated again with a different gas flow. From this initial parameter study, a minimum RF power was identified. This lower limit was used for the rest of the parameter study, as a low power increases the difficulty in igniting and sustaining a plasma.

Table 2: The combination of parameters studied. Starting with the parameters furthest to the left, then decreasing the power along the columns of the table, then repeating with the next pressure, different flow rates were not explored and kept constant at 10 sccm for both CHF_3 and SF_6 .

Power [W]	200	150	100	50	25
Pressure [mTorr]	65	50	40	10	1

However, as will be highlighted in the results section, after completing the first two steps without reaching a point where a plasma could not be generated, it was considered that a brute force method such as this would not be sufficient in finding the limits of the system. Instead, tests were conducted to explore the possibility of generating a plasma at the physical limits of the system (where the chamber conditions are just barely met by the system). As the low limit of power and pressure had already been reached without diminishing plasma production capabilities, the high and low limits of flow rate, as well as the limits of gas ratio had to be considered.

Following this, the gas composition was examined. For low pressures and powers, the ratio of CHF_3 and SF_6 was adjusted in steps of 10 % from 100 % CHF_3 to 100 % SF_6 . The DC bias (and to some extent plasma glow) was used to verify the existence of plasma. Here, the chamber was cleaned between each series of measurements.

Lastly, the very low limits of gas flow were examined, as it was established that low pressure and low power were not limiting factors, at least not in the range of attainable values. This was done by setting the power and pressure to a minimum and increasing the gas flow from 0 sccm and up in integer intervals, turning on the RF power for one minute for each configuration and waiting to see if plasma is created in that time interval. The chamber was here cleaned between every successful plasma

ignition, this time with a shorter process where only an O_2 plasma was used for three minutes. This was done to cut down time, as several plasma ignitions occurred.

3.3 Etching

3.3.1 Sample Preparation and Handling

Three different kinds of samples were etched. Samples with TU7 Resist and Chrome were prepared with Nano Imprint Lithography (NIL). A high resolution sample with AR-P6200 polymer was prepared using electron beam lithography. The samples with Chrome and TU7 both started with applying a double layer of TU7 polymer. This was followed by an imprint step (stamping) of the samples to create the desired pattern, 240 nm wide holes in a square pattern with a 500 nm periodicity. The samples which were to become TU7 mask samples were then hardened while the Cr samples had a deposition of a Cr layer. The TU7 was then removed to expose the Cr layer using a lift off method. This left one sample with holes in TU7 Resist as a mask, and one with Chrome Pillars. The electron beam resist was applied in a similar manner to the TU7, but exposed by an electron beam rather than stamped. This takes a longer time, but allows the creation of smaller features. The samples were then split into pieces which could be etched individually. The procedure of etching and analyzing samples is detailed below.

First, the samples were observed under an optical microscope. This was done to ensure that the pattern was present, and not severely damaged due to previous physical contact. The samples were then placed into 3x3 sample holders such that the chromium samples were in the same row and the samples to be etched for the same time were in the same column.

The patterned samples were attached to an eight-inch Si carrier using a sticky tape, which fixes them in place and improves thermal contact between the carrier and the samples. This wafer is large enough to cover the entire bottom electrode. Once the sample had been placed onto the wafer, the lid was closed and the vacuum engaged. The etching process was carried out as detailed in the next section.

After the samples had been etched, they were again inspected by the optical microscope. The color and brightness of the samples could then be observed to have changed. A deeper etch profile causes a darker observed surface. This step is not necessary, but is useful as an initial indication in what to expect once observing the samples under the SEM.

Following this, the profile of the samples was inspected in the SEM. As the edges of each sample are most likely damaged, the profile of the center of the sample is desired. The samples were cleaved by applying a dent using a sharp object (scalpel or other thin metallic object). The crack was then propagated by applying pressure to the sample when placed on a sharp edge.

Once the sample was cleaved, it was mounted onto a sample holder which clamped the samples into a vertical position, see figure 2.

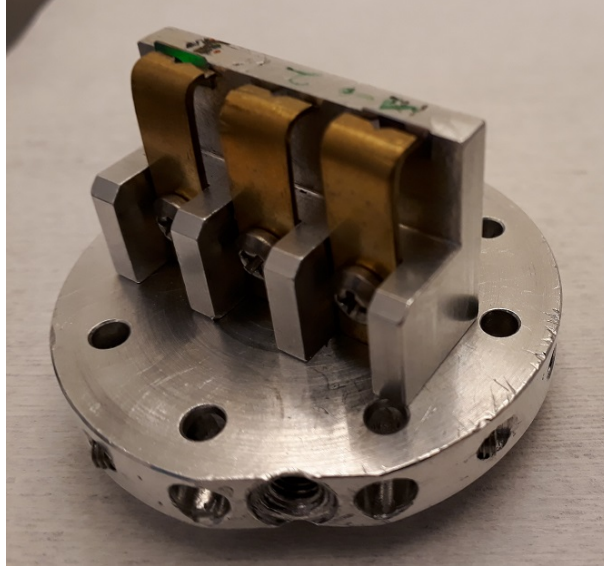


Figure 2: The sample holder with barely visible silicon samples in the clamping device.

The sample holder was then loaded into the SEM load lock and inserted into the SEM where images of the etch profile cross section were taken.

For the High Resolution sample, the half of the sample which was not analyzed in the SEM was then placed in the ellipsometer to measure the mask thickness.

3.3.2 Sample Etching in 8 : 20 sccm of $\text{SF}_6:\text{CHF}_3$

The goal is to achieve highly anisotropic etching of silicon with small feature sizes. The hope is that utilizing the low pressure ranges will yield good results, as has been achieved by previous research teams [11]. The parameters used in their etcher can be seen in Table 3, apart from the RF power where they used 15 W. Additionally, a 4-inch carrier wafer had been used previously, while an 8-inch wafer was used for the etch tests conducted here.

Table 3: The parameters used to etch the first batch of samples. No plasma is generated for the first thirty seconds, as this stage merely exists to pressurize the chamber. Later in the project, a two minute purging process was added as a step three, with 50 sccm of Argon at 500 mTorr and 0 W power.

Etch Procedure Step	1	2
Time	30 s	2 min / 5 min / 10 min
Power [W]	0	25
Pressure [mTorr]	5	5
CHF_3 rate [sccm]	20	20
SF_6 rate [sccm]	8	8

Three samples from each NIL batch were first examined under optical microscope to verify that a repeating pattern could be observed, and that the mask had been correctly deposited. Secondly, the samples were etched for 2, 5, and 10 minutes respectively with a cleaning step in between. Following this, they were viewed under the optical microscope where one could verify that the observed colour of the samples differ as a result of different etch depths, and that this indicated that etching

had occurred. Lastly, the samples were taken to the SEM for imaging, where the etch depth and anisotropy could be measured.

This process was repeated twice with higher RF power, first at 50 W and then at 40 W. This provided enough data to produce some information about the etch rate and selectivity with respect to power (and DC bias) for the system.

3.3.3 Preconditioned Etch Chamber

The previous tests had all been conducted with an initially cleaned chamber. This meant that during the etching process, the plasma could alter the chamber conditions. This could result in unstable plasma which ultimately might alter the etch results. Another test, where the chamber was preconditioned, was suggested. The test was conducted in the same way as previously, but before any etching was done, the chamber was submitted to the desired plasma for 15 minutes in order to guarantee identical conditions during all of the etching process. This test was only conducted on the high power setting (50 W) for two and ten minutes.

3.3.4 Sample Etching in 6 : 24 sccm of SF₆:CHF₃

In order to attempt to increase the selectivity towards resist, the ratio of SF₆ to CHF₃ was reduced from 8 : 20 sccm to 6 : 24 sccm [11]. The idea is that the higher polymerizing agent will prevent sputtering of the mask, while only reducing the etch rate of the silicon slightly.

Unfortunately, in order to preserve time, this test had to be completed immediately following the previous preconditioning test, with no time to clean the chamber in between. This is perhaps not ideal, but was motivated by the fact that the two tests are similar enough that the previous etching would act as a longer preconditioning of the chamber, i.e, previous contamination would have little to no effect on the etching results of the new test. Nevertheless, the chamber was again preconditioned to the new settings in order to minimize the effects of the previous etching.

3.3.5 High Resolution Samples

Lastly, a high resolution sample with trenches in E-beam resist of varying width, from 30 nm to 1 μ m had been prepared. The E-beam resist is less stable than the TU7 resist, which means that the selectivity is likely to be lower. This sample was therefore etched for five minutes at 50 W and 5 mTorr using both of the studied gas flow ratios. The differences in selectivity, minimum dimension width and etch rate against dimension width were examined for both cases.

4 Results and Analysis

Before the results section, it should be noted that measured values are nominal, i.e. the recorded values are those set by the user, not those read during the process. This has an impact on the values for RF power and chamber pressure, where the forward RF power and reflected RF power were displayed (and do not nor should add up to the nominal value). The forward and reflected powers were recorded together with

the nominal power for the parameter study, and can be seen in Table 4. These values remained consistent within an error margin for the etch tests performed later.

Table 4: The nominal power translates to (roughly) these forward and reflected powers. Fluctuations between two integer values were recorded as the half-integer between them.

Nominal Power [W]	Fwd Read [W]	Ref Read [W]
200	186	4
150	137	4
100	87	2
50	38	1.5
25	13	0.5

The readout pressure was also not the same as the nominal pressure, with the system attempting to keep the pressure at 2-3 mTorr lower than the nominal value. For future studies seeking to replicate or further build upon the results in this thesis, these considerations should be reflected upon.

Data plots were generated in python 3 using the matplotlib, and scipy packages.

4.1 Parameter study

The purpose of the parameter study was to find a suitable parameter window within which plasma can be ignited and sustained reliably for the purposes of etching.

The high flow rate limit provided the first limit to this window. This limit was unsurprisingly found with no issues in plasma ignition. Figure 3 shows the measured flow rate limit for various pressures. The measurements have been attributed a flat error of 5 sccm, due to the measurement process.

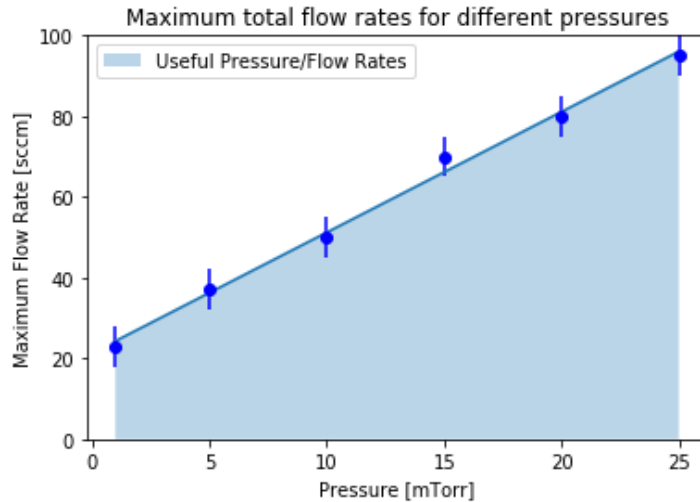


Figure 3: This shows the high limit in flow rate for a range of pressures, a equal amount of $SF_6 : CHF_3$ was used for every measurement.

We can see here that a flow of 35 sccm can be sustained at 5 mTorr with the new pumping capabilities, where previously a flow of 10 sccm could be sustained at 50

mTorr [9].

Conversely, the low flow rate limit test showed that for sufficiently low flow rates, no gas appears to be pumped into the etching chamber. This is likely due to the mass flow control units, which have an accuracy down to a few (1-2) percent. Since their maximum output value is on the order of a hundred sccm, they are expected to fail to control gas flow for single units of flow control. Specifically, it was noted that the lowest possible value for SF₆, and CHF₃ was 3, and 2 sccm respectively. It was also observed that such low flow rates increase the difficulty in igniting the plasma. When using a power of 25 W and 3 sccm of SF₆ flow in a clean chamber, plasma generation was observed to have a delay of up to 40 seconds until a visible plasma glow and a DC bias was detected. A practical limit is therefore placed at 5 sccm for the two gas lines studied.

The power/pressure parameter study did not find any limits to plasma generation. However, it was noted that there was no plasma, DC bias, or recorded power (forward or reflected) in the Trion system when the power was set to less than 25 W. It was assumed that this is a physical limit for the Lund NanoLab Trion system as the transition was very sharp, however, there is a possibility that a weak plasma is generated which does not emit light.

It was also observed that for pressures as low as 1 mTorr, which is the lowest nonzero value setting possible, a plasma was generated with every power setting tested. This suggests that neither power nor pressure have a lower limit in the process window. However, as the system only displays measurements with an integer certainty, setting the pressure to 1 mTorr means a relative error of 100 % in the recorded pressure. It would therefore be advised to select working pressure after the desired tolerances

Furthermore, a somewhat linear trend between power and DC bias could be recorded for several pressures and powers with the specific gas combination used (detailed in table 2), Figure 4. Note that in the etcher itself, the DC Bias is rarely constant, but fluctuates rapidly. The values plotted are therefore estimates. As a general rule, an error of 10 – 15 % is reasonable to assume for these measurements. These fluctuations can vary with gas flow rate and ratio, possibly pressure, and polymer deposition on the bias electrode, where voltage is measured.

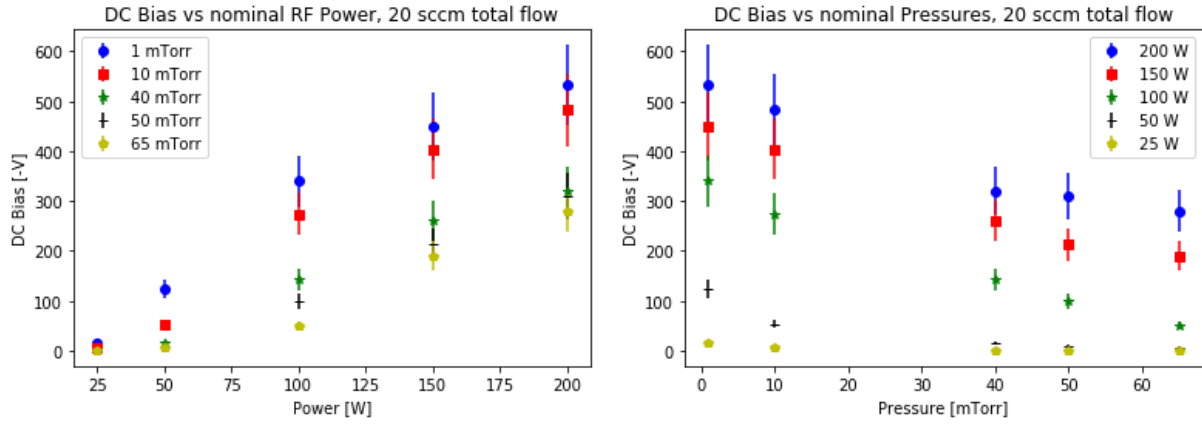


Figure 4: The recorded DC bias for a 10:10 SF₆:CHF₃ ratio for powers ranging between 25 and 200 W and Pressures ranging from 1 to 65 mTorr. The gas flows were kept at 10:10 SF₆:CHF₃ for every measurement

The possibility of gas ratio changing the chamber conditions was explored and it was found that every gas combination tested, at different total flow rates, did provide a stable ignition of the plasma. With the exception being the case where only CHF₃ was used, where the DC Bias fluctuated heavily, to the extent where no single digit could accurately represent it. This could be a hint at an unstable plasma, or that the polymerization hinders proper measurement. Despite this, the plasma glow appeared stable. Apart from this, a trend towards higher DC bias was noticed with higher rates of CHF₃, see Figure 5. This seems to vary very little with total gas flow rate.

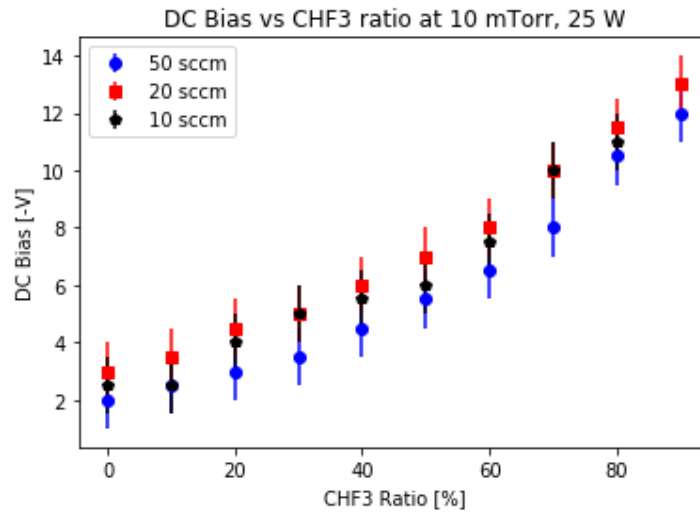


Figure 5: This shows The DC bias as a function of CHF₃ concentration. Increasing CHF₃ rate seems to increase the measured bias, and a 100 % rate produced values with significant fluctuations. Small fluctuations between two integer values were interpreted as half-integer DC bias.

4.2 Etch Tests

4.2.1 Etching in 8:20 sccm of SF₆:CHF₃

The first batch of samples was etched with the settings detailed in Table 3. The SEM was used to capture images where distances could be measured, a subset of which can be seen in Figure 6. It can here be observed that the anisotropy for low power settings is poor, whereas high power settings damage the soft mask heavily.

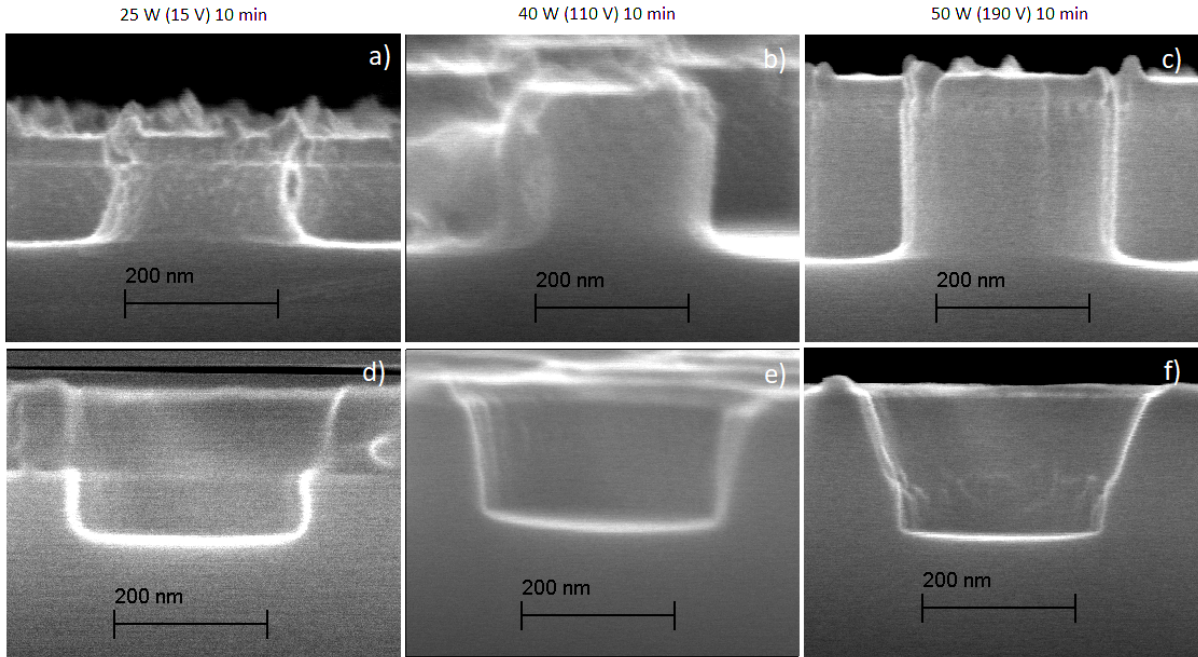


Figure 6: Pillars under the Cr mask (a-c) or holes under the TU7 mask (d-f) respectively, etched for ten minutes at 15, 110, 190 V DC bias, 5 mTorr, and 8:20 sccm of SF₆:CHF₃.

The measurements provided information about etch rates and selectivity and revealed trends for etch rates and selectivity vs power / DC bias. In Figure 7, the etch depths for the two different masks have been plotted against the time they were etched. As expected, with a higher power, comes a higher DC bias which increases the sputtering and etch rates. The plotted trendlines were forced to intersect the origin, as an un-etched sample has no etch depth.

For the TU7 Resist mask, the mask height was also measured with each step. Initially, the mask was measured to be 160 nm thick. The sample etched with high power displayed a large etch rate of the mask. The sample etched for ten minutes displayed no mask, so this data point was not recorded as it is unknown how much the mask would have been etched at that point. The slope was recorded and etch rate computed. This etch rate was compared to the etch rate of silicon in these samples, and the selectivity was plotted in Figure 9. The results indicate that the selectivity is very limited, even for the samples etched at low power. This means that mask thickness has a large impact on the possible etch depths. This can be clearly seen in Figure 6 (f). The sidewalls also have a very noticeable slope. This is probably due to the resist mask being etched away faster at the edges of the mask than at the center.

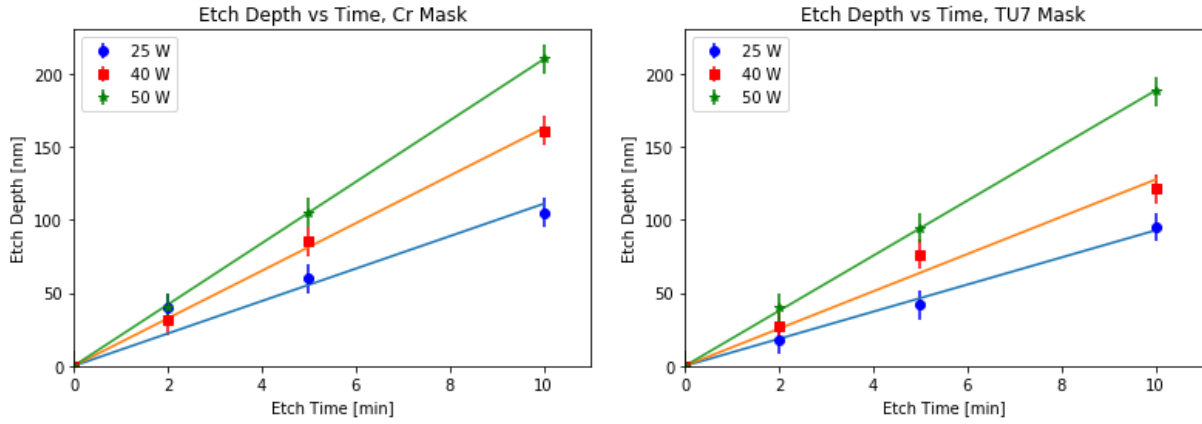


Figure 7: The measured etch depth vs time for silicon samples with a Cr mask (left) and TU7 resist mask (right) at 5 mTorr, and 8:20 sccm of $\text{SF}_6:\text{CHF}_3$. The slopes indicate

The slopes in Figure 7 were measured and plotted against the DC Bias and RF Power (Figure 8) to show how the etch rate increases with increasing bias. It appears that the etch rate for the holes in TU7 resist is consistently slightly lower than the etch rate for pillars under Cr dots. This disparity in etch rate is most likely due to the shape of the pattern, rather than the material of the mask. In a hole, some aperture effects come in, where it becomes increasingly difficult to transport etching material down to the bottom of the hole compared to at the base of a pillar. The polymerization also enhances this effect as the polymer being deposited on the sidewalls decreases the hole diameter. This means that these effects will become more apparent for smaller holes and that the limit in minimum size is larger for holes than pillars.

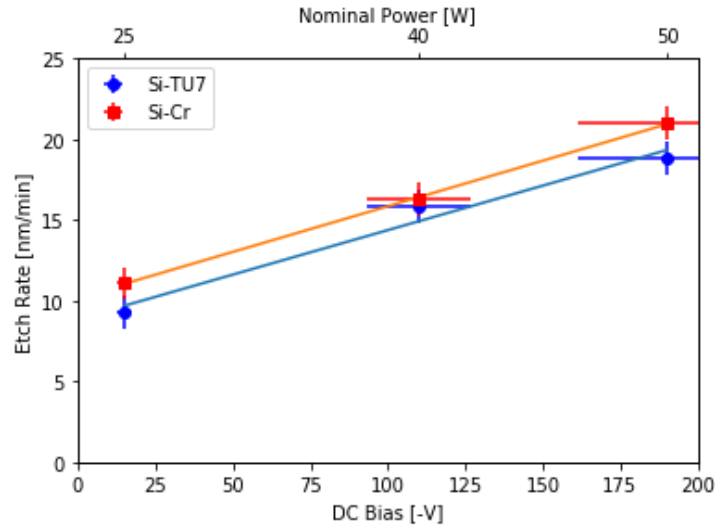


Figure 8: The measured etch rates for Cr and TU7 resist masks depending on DC bias for etch conditions: 5 mTorr, and 8:20 sccm of $\text{SF}_6:\text{CHF}_3$. This information was extracted from the results of Figure 7

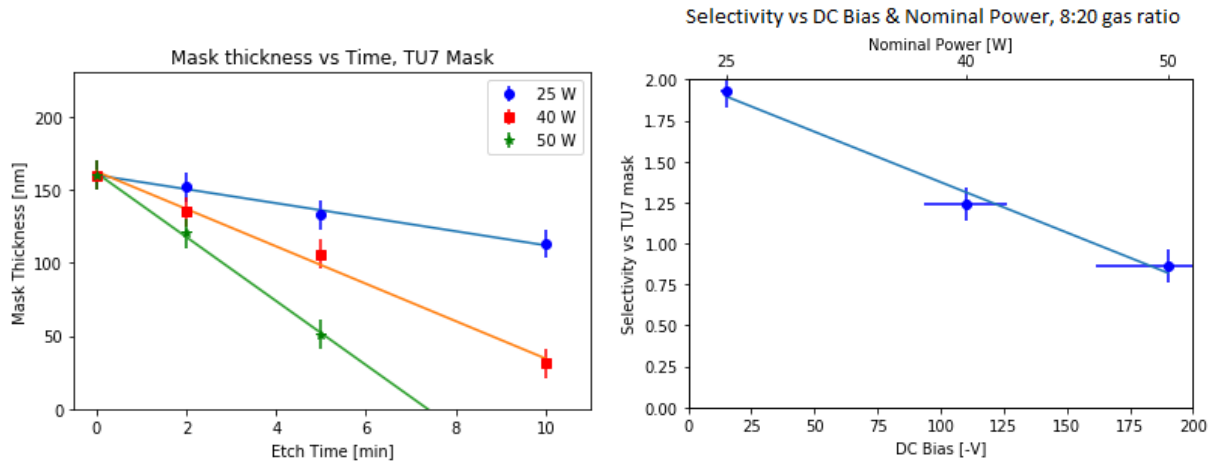


Figure 9: The mask height vs Time for a TU7 resist sample (left). The slopes indicate the etch rate of the mask. The ratio of the silicon etch rate to the mask etch rate was then calculated to find the selectivity (right). The asymmetrical errors stem from the possibility that the mask had melted due to the electron beam.

Quite fortunately, some additional masking material had been present in the Cr mask which resulted in a smaller pillar emerging in the sample etched for five minutes at an intermediate power (40 W), Figure 10. This result suggests that the developed process can be used to etch small features with relatively high aspect ratio and anisotropy, which is a necessary condition for new applications.

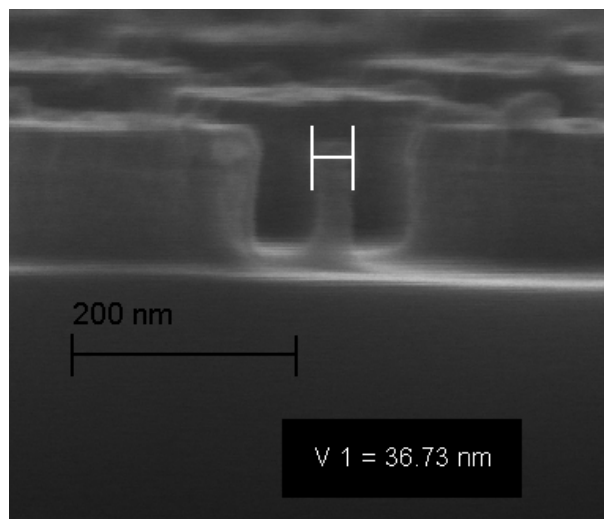


Figure 10: A defect in the mask caused a small pillar to emerge. The pillar was etched for five minutes at 40 W, 5 mTorr, and 8:20 sccm of $SF_6 : CHF_3$. The pillar appears to be around 36 nm wide and 100 nm high. No undercutting can be observed and the sidewalls appear not to slope outwards.

4.2.2 Etching in 6:24 sccm of $SF_6:CHF_3$

The samples with an increased ratio of CHF_3 were also analyzed. It was found that the selectivity did improve by around 75 %, going from 0.86 : 1 to 1.51 : 1. The etch rate also changed, and saw a decrease by 31 %, going from 21.9 nm/min to 15.1 nm/min.

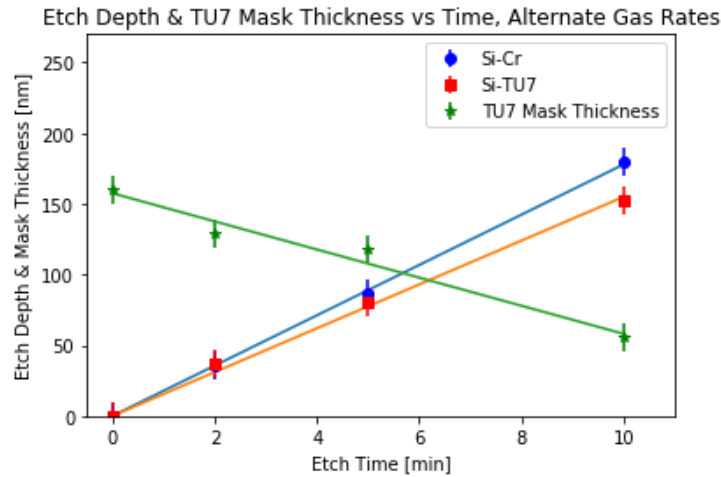


Figure 11: Measurement data for the altered gas ratio 6:24 sccm of $\text{SF}_6:\text{CHF}_3$.

The profile of these samples had also changed a bit, the sidewalls were not observed to be quite as straight, but had a slight slope outwards. Note that, while the sidewalls appear to slope the same in Figure 6 (f) as in Figure 12 (left), the first is due to the mask having been etched away at the sides first, whereas the second one is due to polymerization on the insides. This is confirmed by the difference in width between the two samples. Considering that the holes in the mask are originally 250 nm in diameter, this size is seen at the bottom of the first image, but closer to the top in the second one.

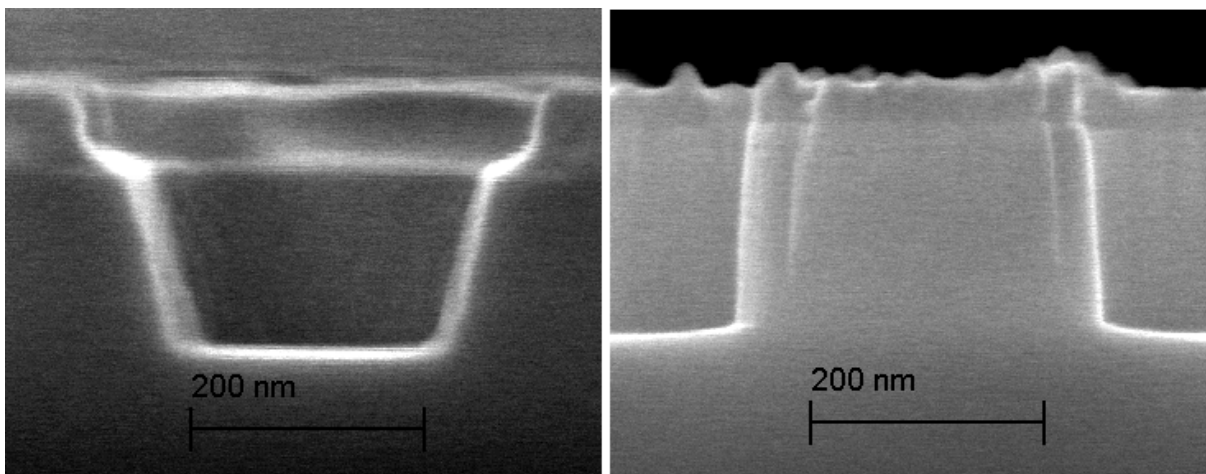


Figure 12: TU7 resist (left) and Cr (right) samples etched with the altered gas ratios (6:24 $\text{SF}_6:\text{CHF}_3$ for 10 minutes at 50 W (180 V DC)).

4.2.3 Preconditioning

The preconditioning test revealed that the effects of preconditioning are negligible on the etch rate, and anisotropy. For a reference, see Figure 13. The samples to the left have been etched in a previously cleaned chamber, whereas the samples to the right were etched in a preconditioned chamber.

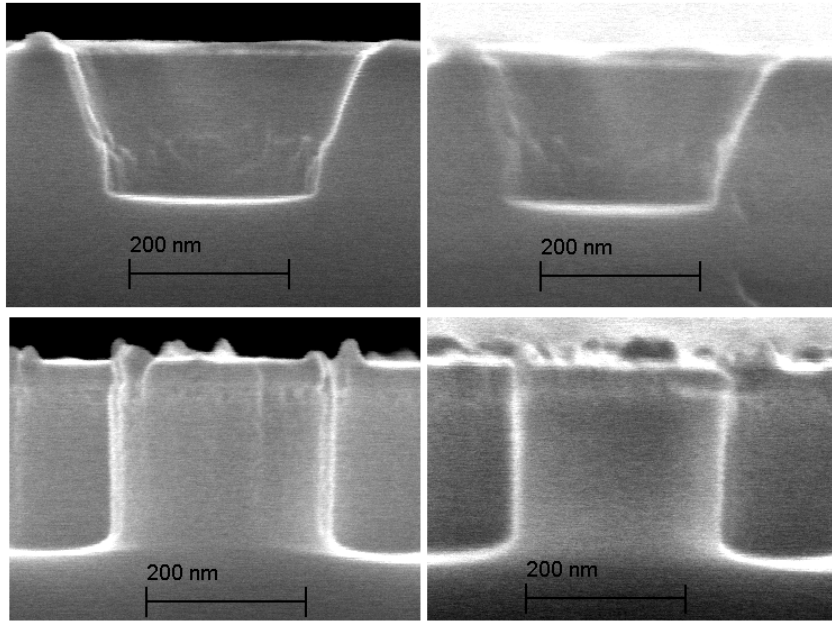


Figure 13: Samples etched in a cleaned chamber (left) and preconditioned chamber (right). Etched for 10 minutes at 50 W, 5 mTorr with 8:20 $SF_6 : CHF_3$ ratio.

4.2.4 High Resolution Lines Sample

Finally, the high resolution samples prepared with electron beam lithography on AR-P6200 resist was etched at 50 W for five minutes using both gas combinations, see figure 14. This gave data on what the smallest dimension etch for each gas was and how the etch rate varied with line width.

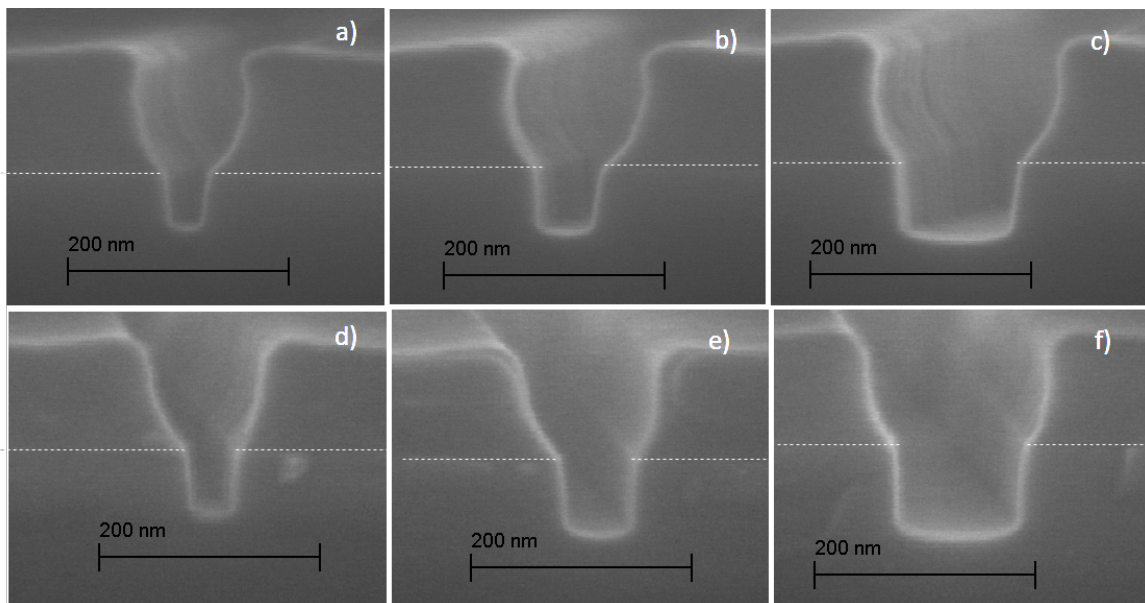


Figure 14: High Resolution etch samples, shown here (left to right) is 30, 50, 100 nm lines, using 50 W, 5 mTorr and gas ratios (top to bottom) 6 : 24 and 8 : 20 sccm of $SF_6 : CHF_3$. The white dotted lines indicate the boundary between Si and masking material.

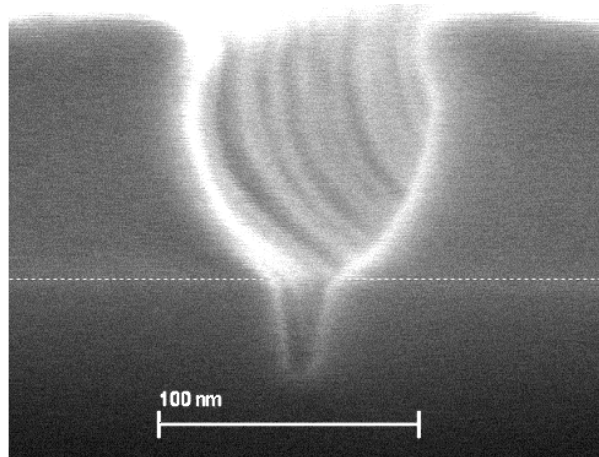


Figure 15: This line was etched to a 33.5 nm depth at a width of 13.9 nm (measured halfway down) at 50 W, 5 mTorr and 6:24 sccm $SF_6 : CHF_3$. The white dotted line indicates the boundary between Si and masking material

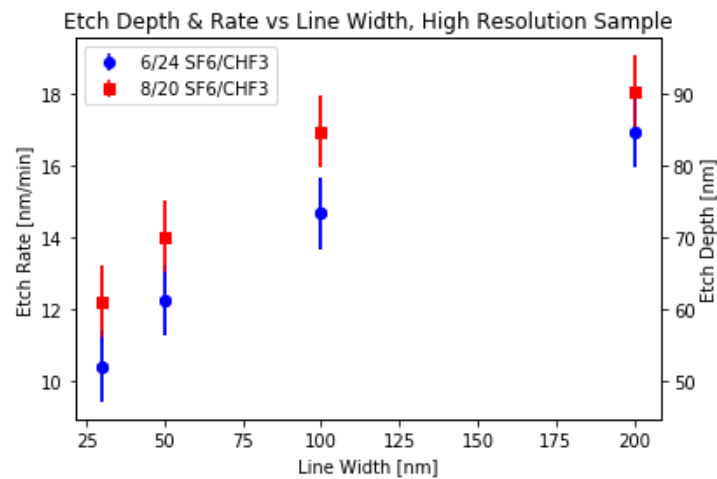


Figure 16: The etch depth obtained for different line widths.

The aperture effect starts making a large difference in etch depth for lines thinner than 100 nm, and completely prevent the 8 : 20 combination from etching the Single Pixel Lines (SPL), which have a width of around 10 nm. Furthermore, there was some observed line widening, particularly for the 8 : 20 configuration, where the resulting etch width is larger than the mask width was originally.

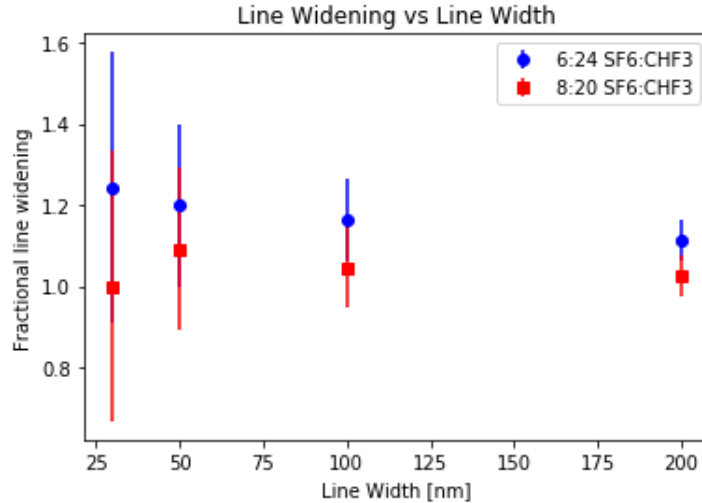


Figure 17: The Fractional increase in line width, defined as the ratio between measured line width and initial mask width

Generally, a widening is observed which decreases with line width, and sees a steep increase for line widths around 30 nm and lower. To note is that the 6 : 24 sample seems to have a lower line widening for every data point. This is likely due to the lower etch speed of the mask, which likely disappears faster near the edges and thus allows the sides to be etched faster.

5 Discussion

5.1 Methodology Errors

During the course of the project, some sources of error could have occurred due to the experimental methods used.

Firstly, it was mentioned that during a moment of the parameter study, the RIE chamber was cleaned using only an O_2 plasma, rather than the combination of O_2 and CF_4 . This was motivated by the fact that the etch test did not include any silicon in the chamber, and thus, there would be no silicon deposited on the side-walls, which is the reason for including CF_4 into the cleaning plasma. Nevertheless, it would have been better to be on the safe side when it comes to matters such as these, since identical chamber conditions were desired for the parameter study.

Another source of possible errors is the reignition effect, where a plasma has an easier time igniting if there has already been a plasma inside. This is likely due to the fact that, after the species ceases to be a plasma, there may still be some excited gas and plasma species remaining. This means that the difficulty of generating a plasma can change depending on previous conditions. This effect ended up being the main cause for the time taken during the parameter study, as the more sensitive regions (low flow rates), had to be separated by a ten minute cleaning step each time a plasma was ignited. Ideally, this cleaning step should have been performed between each plasma ignition during the parameter study, but the time required to do this would have greatly exceeded the time span of this project.

It was also noted that, while a power lower than 25 W seems to abruptly cease plasma ignition, it is possible that a weak plasma is generated and does not glow visibly, as well as not registering in the DC bias detection. To verify whether the power 25 W is a limit, one should attempt etching at lower powers and measure sample heights using an ellipsometer to verify whether a reactive species took place inside or not. This was not done during the course of the project, and the power 25 W was therefore treated as a lower limit.

Additionally, the fact that the time required to clean the chamber is longer for longer etch times, was not considered in the earlier etching stages of the project. This means that there have been stages during the project where the chamber may not have been sufficiently cleaned. Fortunately, the low working pressures means that the rate of polymerization and deposition is quite low, and that errors stemming from this oversight are most likely small. This is supported by the fact that preconditioning seems to have little to no effect on the etching results and that no reflected power was observed.

Lastly, the carrier wafer used in every process was an 8-inch silicon wafer with a crack down the middle (except for the etching of high resolution samples where a new wafer had been produced). Additionally, the wafer was not perfectly clean, and did display some effects of long use. The carrier was still used due to the loading effects described in the methods. Nevertheless, the carrier is not a perfect one, and using a better carrier method could yield improvements upon the methods displayed in this paper. For instance, the sticky tape which, to some extent, are revealed to the plasma, could have been removed in favor of applying a vacuum grease to the bottom of the samples. These improvements were not implemented once discussed, as a significant portion of the etching work had already been done and a change in methods would only serve to make the results inconsistent.

5.2 Measurement Errors

Most important to discuss here is the fact that the DC bias is rarely stable at a single value, but varies in a range of around 10 %. Even this number is no more than an estimate, as the observed variation may depend on other factors, such as gas combination. This can make it difficult to pinpoint a single value to use when creating charts for the analysis of data, especially once higher powers are achieved.

For every etch test, the nominal power of the system was recorded. In reality, the pumping system appears to try to keep the pressure around 2-3 mTorr lower than the nominal (set) value, which does not affect higher pressure ranges too much, but in the lower pressure region, the chamber pressure could easily be half of the nominal value. This provides a soft limit in the system, where different total gas flows will impact the pressure read value. It would probably be wise to use the manual mode to figure out which pressure and gas flow combinations to work with, if specific pressures are desired for an etch process.

The SEM images of the TU7 resist samples were difficult to correctly interpret and to focus on, this being due to the fact that there are no discrete edges, but rather a continuous change in depth along the side walls of the holes. This means that height measurements on this sample are more uncertain than height measurements of the pillars. In fact, the unetched mask height was initially measured to be about 130 nm,

while on a re-examination, the mask height was observed to be 160 nm. This is certainly due to a measurement error in the initial sample, as the mask height has been observed to be larger than 130 nm for some samples etched at low power, in fact, this observation is what spurred the re-measurement of the mask height in the first place.

This does still not guarantee that the mask has been measured properly. The high energy (10 kV) electron beam of the SEM has the ability to melt soft masks. This is likely the reason the mask seems to have been hollowed out around holes or lines. In the worst case scenario, this effect could also have reduced the mask height, which means that calculated selectivities could be lower an upper estimate places this mask height reduction at up to 30 %, however, no measurement has been made to verify this guess. Since it is difficult to quantify this effect without taking measurements with this in mind, and this concern was raised late into the project, this effect has not been represented in the results section.

6 Conclusion and Outlook

The parameter study revealed that the process window for etching in the LNL RIE is limited by high flow rates as seen in figure 3 and for practical purposes, flow rates under 5 sccm should be avoided. No limit was observed due to pressure, where plasma could be generated at 1 mTorr with no issue. The limiting factor in pressure should therefore be which uncertainty in pressure is acceptable, as the measured pressure is only accurate up to one digit. Lastly, the power appears limited by the system at 25 W.

The etch tests revealed that etching anisotropic structures at low pressures is definitely possible. Figure 10 shows that pillars as small as 35 nm can be etched with high anisotropy. Unfortunately, the etch rates and selectivities are currently too limited for practical applications using soft masks, or any type of deep etching. With etch rates ranging from 11 nm/min to 21 nm/min and selectivities between 0.9 and 1.9. A high etch rate leads to a low selectivity and vice versa. Ideally, etch rates above 20 nm/min and selectivities around 2:1 would be desired. Practically, the "best" combination was a rate of 15 nm/min and selectivity 1.5:1, seen with a higher rate of polymerizing gas (6:24 SF_6 : CHF_3). Using a hard mask, the selectivity was not a concern, in which case the etch rates would suffice and could likely be improved further by increasing etching power until substrate damage occurs.

Lastly, the high resolution samples showed that lines as narrow as 15 nm can be etched with low etch rates. It was found that aperture effects start making a large difference in etch rates for structures smaller than 200 nm wide, with drastic decreases for structures smaller than 100 nm. It was also noted that a larger ratio of fluorine to carbon appears to contribute to a certain line widening.

Future research into the etch processes developed could focus on altering gas ratios and power, or introducing new gas species into the mixture in order to increase etch rates and selectivity. The dependency on pressure regarding etch rates, isotropy and selectivity was also not investigated, and the possibility exists that increasing the pressure does not hurt the anisotropy while benefiting etch rates and thus selectivity. Suggested improvements of the methods used in this study are to use an ellipsometer to measure mask height for more consistent measurements of the selectivity.

The results of this project show some promise for future applications, the trench with a width of 15 nm has dimensions roughly equal to the size of a modern transistor, which suggests that some improvements to the methods covered in this thesis could see applications in the manufacturing of transistors, for instance. The 35 nm wide pillar also shows that anisotropic structures can be developed for high resolution NIL stamps.

7 Acknowledgements

I want to thank everyone who was involved in the work behind this thesis, in particular Ivan Maximov for supervising the project and Mariusz Graczyk, Dmitry Suyatin, and Anders Kvennefors for taking their time to teach me how to use the various tools that have been utilized in the production and analysis of data, as well as producing the samples which were analyzed. Lastly, I want to thank my family and friends who have been supportive and encouraging over the course of the project.

References

- [1] R. G. Poulsen, Plasma etching in integrated circuit manufacture — A review. *Journal of Vacuum Science and Technology* 14, 266 (1977); <https://doi.org/10.1116/1.569137>
- [2] Vincent M. Donnelly and Avinoam Kornblit, Plasma Etching: Yesterday, Today, and Tomorrow. *Journal of Vacuum Science & Technology A* 31, 050825 (2013); <https://doi.org/10.1116/1.4819316>
- [3] Yin Y, Bilek M, McKenzie D. The origins of self-bias on dielectric substrates in RF plasma processing. *Plasma Sources Sci. Technol.* 22 065013 (2013); <https://doi.org/10.1088/0963-0252/22/6/065013>
- [4] Alfred Grill. *Cold Plasma in Materials Fabrication - From Fundamentals to Applications*. Chapters 1-3, 8. IEEE PRESS 445 Hoes Lane, PO Box 1331 Piscataway, NJ 08855-1331, (1993)
- [5] Daniel. L. Flamm, Mechanisms of silicon etching in fluorine- and chlorine-containing plasmas. *Pure & Appl. Chem.*, Vol. 62, No. 9, pp. 1709-1720, (1990)
- [6] J. W. Coburn and Harold F. Winters. Ion- and electron-assisted gas-surface chemistry - An important effect in plasma etching. *Journal of Applied Physics* 50, 3189 (1979); <https://doi.org/10.1063/1.326355>
- [7] <http://triontech.com/etch-platform/sirus-rie/>
- [8] Deep anisotropic silicon etching in TRION RIE - Mariusz Graczyk
- [9] Personal Correspondence with Mariusz Graczyk
- [10] E. Gogolides, S.Grigoropoulos, A.G.Nassiopoulos. Highly anisotropic room-temperature sub-half-micron Si reactive ion etching using fluorine only containing gases (1995) [https://doi.org/10.1016/0167-9317\(94\)00143-I](https://doi.org/10.1016/0167-9317(94)00143-I)
- [11] Personal Correspondence with Andrea Cattoni